

# Nuclear Effects in Electron Capture into Highly Charged Heavy Ions

W. Scheid<sup>1</sup>, A. Pálffy<sup>2</sup>, Z. Harman<sup>2</sup>, C. Kozhuharov<sup>3</sup>, and C. Brandau<sup>3</sup>

<sup>1</sup> Institut für Theoretische Physik der Justus-Liebig-Universität Giessen, Germany

<sup>2</sup> Max-Planck-Institut für Kernphysik, Heidelberg, Germany

<sup>3</sup> Gesellschaft für Schwerionenforschung m.b.H., Darmstadt, Germany

**Abstract.** If a free electron is captured into the K- or L-shell of few-electron heavy ions, several resonance effects can be studied: dielectronic recombination, where the energy of the captured electron is transferred to excite a bound electron, and nuclear excitation by electron capture, where the energy of the free electron is used to excite the nucleus. The dielectronic recombination shows effects of the Breit interaction, the exchange of a virtual transverse photon between the electrons. With the dielectronic recombination, shifts of the resonance lines due to the nuclear charge distributions are investigated. The process of nuclear excitation by electron capture can be applied to explore properties of excited nuclear states.

## 1 Introduction

The capture of a free or quasi-free electron into the inner shells of a highly charged heavy ion can be influenced by the atomic nucleus. One can think of two main effects: 1. the electric potential of the nucleus deviates from the pure Coulomb potential which results in an isotope shift of the resonance lines observed in the capture of an electron. 2. The nucleus can be excited and then it de-excites radiatively to its ground state. In the following we describe these effects in detail.

If a free or quasi-free electron recombines into the bound states of an ion, several processes can occur: The energy difference between the continuum and bound states, set free by the electron, can be irradiated in the emission of a photon. This process is the radiative recombination (RR). The energy can be also transferred to a bound electron which gets excited. The excited atomic system decays by photo – emission in the next step. The latter two-step process is resonant and is called dielectronic recombination (DR). The energy difference can also be used to excite the atomic nucleus, denoted as nuclear excitation by electron capture (NEEC). The excited nucleus has the possibility to de-excite to its ground state by internal conversion (IC) or radiatively by the emission of a photon. Further processes following the capture of a free electron into a bound state may be considered.

In Section 2 we compare recent measurements [1] of KLL dielectronic recombination at GSI (Darmstadt, Germany) with theoretical predictions. In Section 3 we demonstrate the sensitivity of dielectronic resonance lines to the radius of the nuclear charge-distribution observed in recent experiments [2] at GSI. Sections 4 and 5 give a discussion about nuclear excitation by electron capture which is not yet measured [3–6].

## 2 The Breit Interaction in KLL Dielectronic Recombination

The major aim of our investigations is the study of the interaction between electrons in transitions between deeply bound states in highly charged heavy ions. Here, we have to consider a current-current interaction and retardation effects besides the usual Coulomb interaction in transversal gauge. The additional interactions arise due to the exchange of a transverse virtual photon with an energy  $\hbar\omega$  between the electrons and are denoted as Breit interaction.

The generalized Breit interaction is given by

$$V_{12}^{GBI} = e^2 \left( -\boldsymbol{\alpha}_1 \boldsymbol{\alpha}_2 \frac{\cos(\omega r_{12}/c)}{r_{12}} + (\boldsymbol{\alpha}_1 \nabla_1)(\boldsymbol{\alpha}_2 \nabla_2) \frac{\cos(\omega r_{12}/c) - 1}{(\omega/c)^2 r_{12}} \right), \quad (1)$$

where  $\boldsymbol{\alpha}_1$  and  $\boldsymbol{\alpha}_2$  are the Dirac matrices of the electrons. In the limit  $\omega \rightarrow 0$  one obtains the usual Breit interaction

$$V_{12}^{BI} = \lim_{\omega \rightarrow 0} V_{12}^{GBI} = -\frac{e^2}{2r_{12}} \left( \boldsymbol{\alpha}_1 \boldsymbol{\alpha}_2 + \frac{(\boldsymbol{\alpha}_1 \mathbf{r}_{12})(\boldsymbol{\alpha}_2 \mathbf{r}_{12})}{r_{12}^2} \right). \quad (2)$$

Using the transversal gauge, one derives the cross section for photo recombination (e.g. RR and DR) from the Hamiltonian [7]

$$H = H_e + H_r + H_{er} \quad (3)$$

with the electronic part

$$H_e = \sum_{i=1}^N (c\boldsymbol{\alpha}_i \mathbf{p}_i + (\beta_i - 1)mc^2 + V_{Coul}(r_i)) + \sum_{i=1}^N \sum_{j=i+1}^N \frac{e^2}{|r_i - r_j|}, \quad (4)$$

the radiation field part

$$H_r = \sum_{\mathbf{k}\lambda} \hbar\omega_k a_{\mathbf{k}\lambda}^\dagger a_{\mathbf{k}\lambda} \quad (5)$$

and the interaction between the electrons and the radiation

$$H_{er} = \sum_{i=1}^N \sum_{\mathbf{k}\lambda} ec \sqrt{\frac{2\pi\hbar}{L^3\omega_k}} \boldsymbol{\alpha}_i \boldsymbol{\varepsilon}(\mathbf{k}, \lambda) (\exp(i(\mathbf{k}\mathbf{r}_i - \omega_k t)) a_{\mathbf{k}\lambda} + c.c.). \quad (6)$$

The total cross section for DR is obtained with the method of Feshbach introducing subspaces with the ion in its initial state and the initially free electron, with the intermediate states  $d$  and with the final states and the emitted photon:

$$\sigma_{fi}^{DR} = \frac{\pi\hbar^2}{p^2} \sum_d \frac{2J_d + 1}{2(2J_i + 1)} \frac{\Gamma^A(d \rightarrow i)\Gamma^R(d \rightarrow f)}{(E - E_d)^2 + \Gamma_d^2/4}. \quad (7)$$

Here,  $\Gamma^A$  and  $\Gamma^R$  are the Auger and radiative widths of the intermediate states  $d$ , respectively,  $\Gamma_d = \Gamma^A + \Gamma^R$  is approximately the width of the intermediate state,

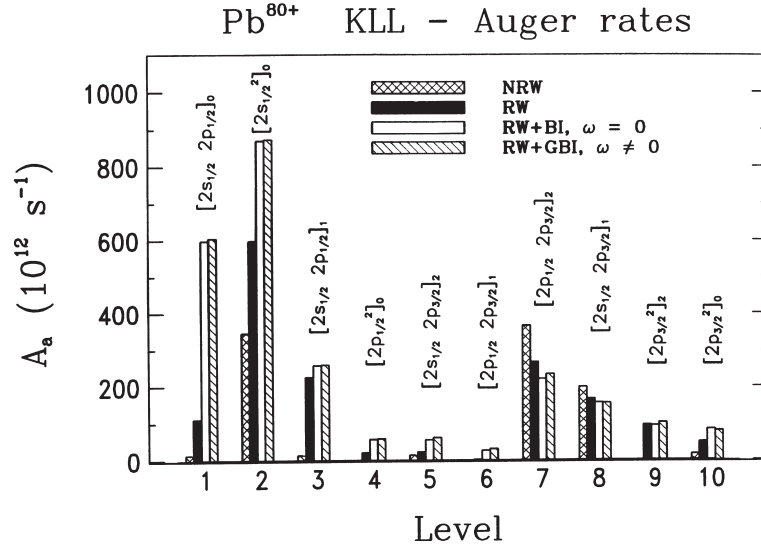


Figure 1. KLL-Auger rates of He-like  $\text{Pb}^{80+}$  for all two-electron levels of the L shell. The crossed and full bars represent rates calculated with nonrelativistic (NRW) and relativistic (RW) wave functions, respectively. The empty and dashed bars represent rates calculated with relativistic wave functions by taking into account the usual ( $\omega = 0$ ) (BI) and the general ( $\omega \neq 0$ ) (GBI) Breit interaction, respectively.

$E_d$  is the energy of the intermediate state and  $p$  the momentum of the initially free electron. The Auger widths are calculated by taking into account the Breit interaction. The wave functions of the bound states are obtained with a multi-configuration Dirac-Fock method in the framework of the General Relativistic Atomic Structure Programme (GRASP) of Dylla, Grant *et al.* [8].

In DR the following notation is introduced: KLL (or KLM) means capture of a free electron into the L(M) shell with a simultaneous excitation of the bound electron from the K-shell to the L-shell. As examples we show the KLL-Auger rates of  $\text{Pb}^{80+}$  in Figure 1 [9]. The decaying state has two electrons initially in the L-shell where 10 states can be formed serving as resonant intermediate states in DR. These 10 states can be classified in three energetically separated groups depending on the angular momentum of the electrons:  $\text{KL}_{1/2}\text{L}_{1/2}$ ,  $\text{KL}_{1/2}\text{L}_{3/2}$ ,  $\text{KL}_{3/2}\text{L}_{3/2}$ . The first group ( $\text{KL}_{1/2}\text{L}_{1/2}$ ) contains four states which are very sensitive to the Breit interaction as demonstrated in Figure 1 [9]. About 40% of the contributions to the Auger rates of the resonances of the  $\text{KL}_{1/2}\text{L}_{1/2}$  group arise from the Breit interaction. A similar effect one observed in resonant capture of a quasi-free electron in collisions of  $\text{U}^{90+}$  on graphite measured with the Experimental Storage Ring of GSI [10, 11].

Figure 2 shows the DR rate coefficient for KLL-DR on  $\text{U}^{91+}$  measured by Brandau, Kozhuharov, Müller *et al.* [1] at GSI. The resonances within the groups can not yet be resolved. The full curve shows a calculation including the Breit interaction playing a major role only in the  $\text{KL}_{1/2}\text{L}_{1/2}$  group.

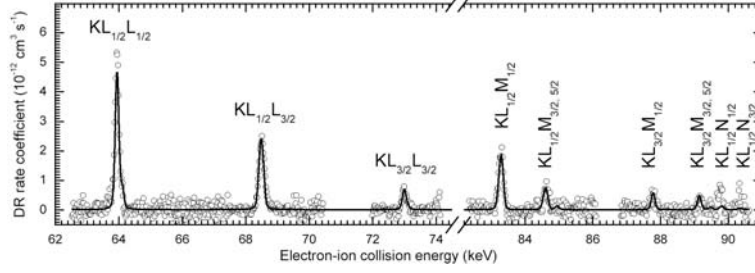


Figure 2. Comparison of theory (solid line) and measurement (circles) of the DR rate coefficient for DR into  $U^{91+}$  as a function of the energy of the electron [1].

### 3 Isotope Shifts of Dielectronic Resonance Lines for Heavy Few-Electron Ions

The finite charge distribution of the nucleus leads to a measurable shift of the resonance energies in dielectronic recombination with few-electron heavy ions. If a series of isotopes is compared, one obtains an isotope shift of the dielectronic resonance lines [2, 12].

The position of the Lorentz peak in (7) depends on the energies of the initial and intermediate states which are affected by isotope effects. Isotope shifts are slight variations of the electronic energies without splitting. These shifts arise mainly due to the volume effect by an isotopic change of the charge distribution of the nucleus and due to a change of the nuclear mass in isotope series. The mass shift contribution in the considered heavy ions is about 2 – 6 orders of magnitude smaller than the volume shift.

For the calculation of the volume shift we assumed a spherical charge distribution in form of a two-parameter Fermi distribution. We used the following root mean square (RMS) radius for a given mass number  $A$ :

$$r_{RMS} = (0.836A^{1/3} + 0.570) \text{ fm} \quad (8)$$

and a fixed surface thickness parameter  $t = 2.30$  fm over which the density decreases from 90% to 10% of its maximum. Calculations of isotope shifts were performed for relativistic ions in the range from  $Z = 54$  to 94 for H-, He- and Li-like ions. In Figure 3 we show the dependence of the isotope shift of resonance energies on the charge number for selected resonances for KLL-DR into H-like ions. The shift is calculated as the difference between the resonance energies for an isotope with a given mass number  $A$  and for  $A - 5$ , respectively:

$$\Delta E_{res}(Z, A) = E_{res}(Z, A - 5) - E_{res}(Z, A). \quad (9)$$

The mass number  $A$ , corresponding to a stable isotope, is obtained by inverting the semi-empirical formula

$$Z = \frac{A}{1.98 + 0.015A^{2/3}} \quad (10)$$

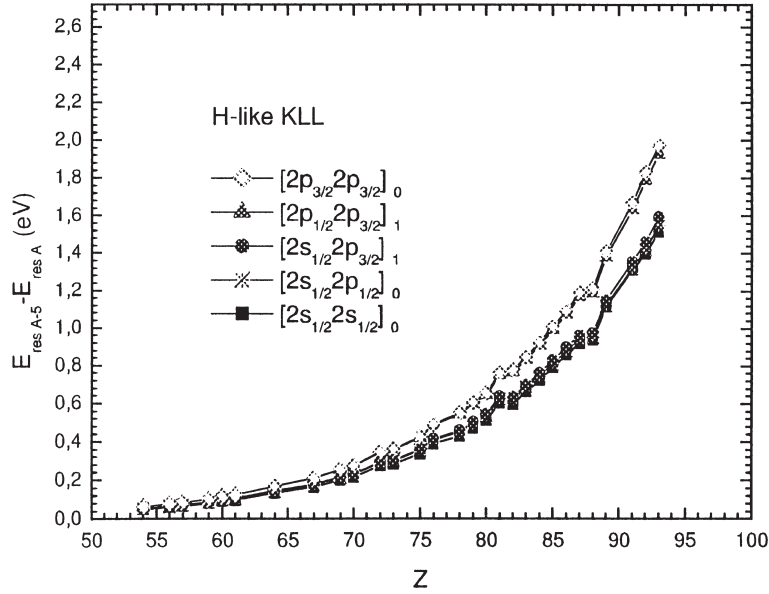


Figure 3. Difference between the resonance energies of two different isotopes with mass numbers  $A$  and  $A - 5$  in the case of KLL DR into H-like ions as a function of the charge number (from Ref. [12]).

and rounding the mass number  $A$  to an integer value. The  $Z$  dependence of the isotopic energy shifts of 5 selected resonances out of the 10 possible ones is shown in Figure 3. In ions with higher charge numbers, the electronic probability density has a larger overlap with the nuclear charge and the result is a more pronounced nuclear volume effect.

Figure 4 shows the measured isotope shift in the DR of Li-like  ${}^A\text{Nd}^{57+}$  with  $A = 142$  and  $A = 150$  [2]. From the displacement of the resonance position the energy shifts  $\delta E^{142-150}(2s - 2p_{1/2}) = 40.2$  meV and  $\delta E^{142-150}(2s - 2p_{3/2}) = 42.3$  meV of the  $2s - 2p_j$  transitions were deduced. An evaluation of these values within a full QED treatment yielded a change in the mean square charge radius of  ${}^{142-150}\delta\langle r^2 \rangle = -1.36$  fm<sup>2</sup>. This approach combines the advantage of a relatively simple atomic structure with a high sensitivity to the nuclear size.

#### 4 Nuclear Excitation by Electron Capture

Nuclear excitation by electron capture (NEEC) is the nuclear physics analogue of DR [3–5]. Instead of the excitation of a bound electron, the energy of the free electron is transferred to the nucleus. If the electronic and nuclear energy levels match, the recombination can take place with the simultaneous excitation of the nucleus. After NEEC, the excited nucleus de-excites by radiative decay or by internal conversion (IC). The IC is the time-inverted process of the NEEC.

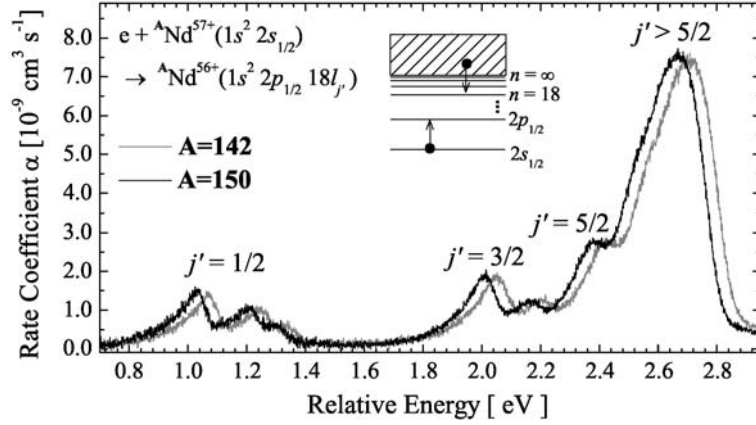


Figure 4. Measurement of dielectronic recombination of the Li-like isotopes  $^{142}\text{Nd}^{57+}$  (gray line) and  $^{150}\text{Nd}^{57+}$  (black line) in the energy range of the  $1s^2 2p_{1/2} 18l_{j'}$  resonance groups. The labels indicate the individual fine structure components  $j'$  of the  $n = 18$  Rydberg electron (from Ref. [2]).

The determination of the cross section for NEEC proceeds similarly to the calculation of the DR cross section. The capture rate is determined by the electric and magnetic interaction of the captured electron and the nucleus:

$$H_{int} = -e \int d^3 r_n \frac{Q_n(\mathbf{r}_n)}{|\mathbf{r}_e - \mathbf{r}_n|} + \frac{e}{c} \alpha \int d^3 r_n \frac{\mathbf{j}_n(\mathbf{r}_n)}{|\mathbf{r}_e - \mathbf{r}_n|}, \quad (11)$$

where  $Q_n(\mathbf{r}_n)$  is the operator for the nuclear charge density and  $\mathbf{j}_n(\mathbf{r}_n)$  the operator of the nuclear current density. With  $H_{int}$  and a model for the nuclear dynamics one can calculate the corresponding capture rate  $Y_n^{i \rightarrow d}$ . In order to get reliable rate values, we inserted experimental values of the electromagnetic transition probabilities of the considered nuclei, namely  $B(EL)$  and  $B(ML)$  values. The cross section for NEEC can be written in analogy with the cross section for DR, given in (7),

$$\sigma_{i \rightarrow d \rightarrow f}^{NEEC}(E) = \frac{\pi \hbar^3}{p^2} \frac{Y_n^{i \rightarrow d} \Gamma_n^R(d \rightarrow f)}{(E - E_d)^2 + \Gamma_d^2/4} \quad (12)$$

with the electron capture rate  $Y_n^{i \rightarrow d}$  and the radiative transition width of the nucleus  $\Gamma_n^R(d \rightarrow f)$ . The natural width of the intermediate state (excited nuclear state) is  $\Gamma_d = \sum_f (\Gamma_n^R(d \rightarrow f) + \Gamma^{IC}(d \rightarrow f))$ , where  $\Gamma^{IC}$  is the width with respect to the internal conversion process. The dimensionless IC coefficient is given by  $\alpha = \Gamma^{IC}(d \rightarrow f)/\Gamma_n^R(d \rightarrow f)$  where  $f$  means the nuclear ground state. Usually one presents the resonance strength defined as [3]

$$S_d = \int dE \sigma_{i \rightarrow d \rightarrow f}^{NEEC}(E) = \frac{2\pi^2 \hbar^3}{p^2} \frac{Y_n^{i \rightarrow d} \Gamma_n^R(d \rightarrow f)}{\Gamma_d}. \quad (13)$$

In even- $A$  nuclei mainly  $E2$ -transitions are possible whereas odd- $A$  nuclei allow  $M1$ -transitions. We calculated NEEC into bare or He-like ions, considering the  $E2$ -transitions in the  $^{154}\text{Gd}$ ,  $^{156}\text{Gd}$ ,  $^{162}\text{Dy}$ ,  $^{164}\text{Dy}$ ,  $^{170}\text{Er}$ ,  $^{174}\text{Yb}$ ,  $^{236}\text{U}$ ,  $^{238}\text{U}$  and  $^{248}\text{Cm}$  nuclei, and the  $M1$ -transitions in the  $^{55}\text{Mn}$ ,  $^{57}\text{Fe}$ ,  $^{155}\text{Gd}$ ,  $^{165}\text{Ho}$ ,  $^{173}\text{Yb}$ ,  $^{185}\text{Re}$  and  $^{187}\text{Re}$  nuclei.

Table 1. Resonance strengths  $S_d$  for NEEC followed by photon emission.  $E_n$  is the nuclear excitation energy and  $\Gamma_d$  is the width of the excited nuclear state. For further information see Ref. [3].

Isotope	$E_n$ (keV)	Type	$Y_n$ (1/s)	$\Gamma_d$ (eV)	$S_d$ (beV)
$^{174}\text{Yb}$	4.89	$E2$	$1.79 \times 10^8$	$4.85 \times 10^{-8}$	0.09
$^{173}\text{Yb}$	7.07	$M1$	$7.32 \times 10^9$	$4.80 \times 10^{-6}$	1.26
$^{185}\text{Re}$	42.19	$M1$	$2.62 \times 10^{10}$	$2.36 \times 10^{-5}$	1.34
$^{187}\text{Re}$	51.08	$M1$	$2.50 \times 10^{10}$	$2.47 \times 10^{-5}$	1.16

The total cross sections have the shape of a very narrow Lorentzian, with the width given by the natural width of the nuclear excited state, which is in the order of  $10^{-5} - 10^{-8}$  eV, and the resonance strength of about 1 beV or less. In Figure 5 we present the total cross section for NEEC followed by the  $M1$  radiation decay of the nucleus in the case of  $^{185}\text{Re}$  as a function of the energy of the continuum electron. This isotope has the largest NEEC resonance strength, namely,  $S = 1.34$  beV for the capture into the  $1s$  orbital. This value is small in comparison with the DR resonance strengths, which are observed experimentally on the order of  $10^3$  beV. NEEC is a

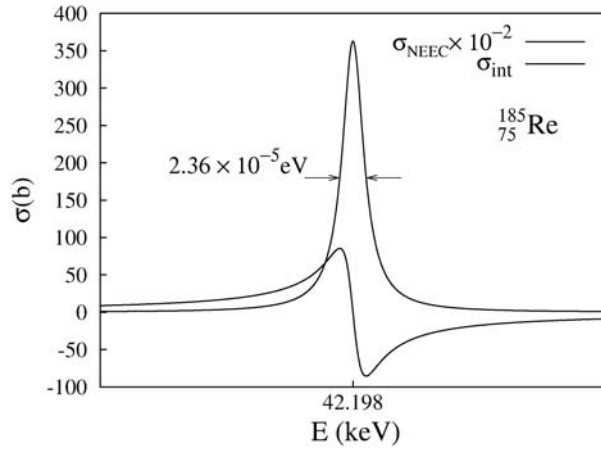


Figure 5. NEEC cross section for capture into bare  $\text{Re}^{75+}$  ions as a function of the continuum electron energy. Also shown is the interference term of the NEEC followed by radiative decay of the nucleus with the RR. The NEEC cross section is scaled by a factor of  $10^{-2}$ .

slow process in comparison to DR and RR because of the relatively long lifetime of the excited nuclear state.

The NEEC process is not yet observed. An experimental energy resolution of less than 1 eV is required for the continuum electron in order to measure the NEEC effect. In addition we investigated the role of RR in the NEEC recombination mechanism and calculated the interference between these two processes. The second curve in Figure 5 gives the interference term, which is negligibly small compared to the NEEC cross section [4]. Also we considered the angular distribution of radiation emitted following NEEC [5].

## 5 Prolongation of Lifetimes of Excited Nuclear States

The integrated cross section of NEEC followed by the  $\gamma$ -decay of the nucleus can be significantly increased in highly charged ions if the resonant capture proceeds via the states of the L-shell with a following fast x-ray decay of the electron from the L-shell to the K-shell (NEECX) [6]. The different steps of this process are presented in Figure 6 for the electron capture into the L-shell of an initially bare ion. Since the transition of the electron between the L- and K-shells is in general faster than the nuclear de-excitation by IC or by radiative transition, the electron decays fast into the K-shell and can no longer be used for the IC process. Thus, the excited nucleus can only decay radiatively to its ground state. This prolongs the lifetime of the excited nucleus.

In the case of  $^{238}_{92}\text{U}$  and  $^{232}_{90}\text{Th}$  actinide nuclei the low-lying  $2^+$  excited nuclear states have energies  $E_{2^+} = E_\gamma = 44.910$  keV and 49.369 keV, respectively, connected via an  $E2$  transition with the nuclear ground state. Due to the large binding energy of the K-shell electron,  $-131.815$  keV for  $\text{U}^{91+}$  and  $-125.248$  keV for  $\text{Th}^{89+}$ , the decay of the first excited nuclear state by IC of the 1s electron is forbidden. The lifetimes of the L-shell one-electron configurations of a  $\text{U}^{91+}$  ion are

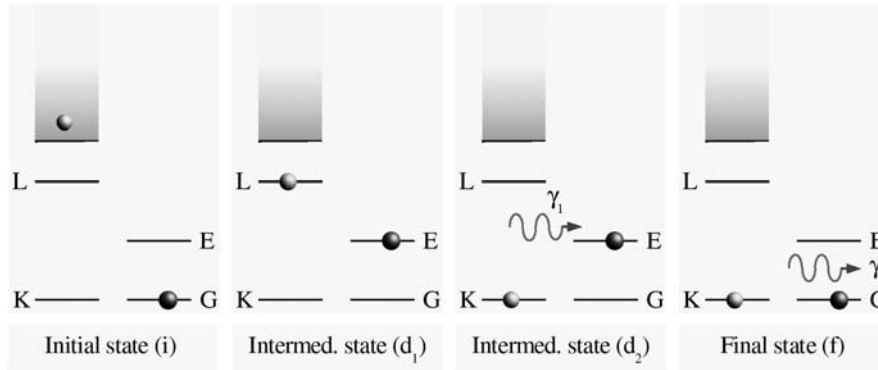


Figure 6. Schematic representation of the three-step process of NEECX followed by the radiative decay of the nucleus.



$5 \times 10^{-15}$  s,  $2 \times 10^{-17}$  s and  $3 \times 10^{-17}$  s for the  $2s$ ,  $2p_{1/2}$  and  $2p_{3/2}$  orbitals, respectively. For comparison, the nuclear excited state lives approximately  $2 \times 10^{-10}$  s in the case of neutral atoms. Similar numbers apply for  $\text{Th}^{89+}$ . The L-shell electron will therefore de-excite rapidly to the K-shell, leading to an intermediate state  $d_2$  (see Figure 6), consisting of the electron in the K-shell and the excited nucleus. Since IC is forbidden, the nucleus has to de-excite radiatively, and its lifetime is given by the  $\gamma$ -decay rate,  $\tau_\gamma = A_\gamma^{-1}$ .

The resonance strength of this process is given by

$$S_{NEECX}^{i \rightarrow f} = \frac{2\pi^2 \hbar^5}{p^2} \frac{A_{rad,n}^{d_2 \rightarrow f}}{\Gamma_{d_2}} \frac{A_{rad,e}^{d_1 \rightarrow d_2}}{\Gamma_{d_1}} Y_n^{i \rightarrow d_1}, \quad (14)$$

where  $d_1$  denotes the doubly-excited state after NEEC and  $d_2$  the singly-excited state with the electron in the K-shell. The widths are  $\Gamma_{d_1} \approx \Gamma_{rad,e}$  and  $\Gamma_{d_2} = \Gamma_{rad,n}$ . In Table 2 we compare resonance strengths for He-, Be-, and C-like ions with those for bare ions with a fast x-ray transition. One can recognize an increase by two orders of magnitude. Table 3 presents the mean-lives for the first excited nuclear

Table 2. Resonance strengths for NEEC and NEECX followed by the radiative decay of the nucleus. In the third column,  $S_{NEEC}$  is the resonance strength for NEEC into the  $2s_{1/2}$  orbital of initially He-like ions,  $2p_{1/2}$  orbital of Be-like ions and  $2p_{3/2}$  orbital of C-like ions, respectively, calculated following the formalism described in Ref. [3].  $S_{NEECX}$  is the resonance strength of NEECX into bare ions. The capture orbital is denoted by  $nl_j$ .

$\frac{A}{Z}X$	$nl_j$	$S_{NEEC}$ (b eV)	$S_{NEECX}$ (b eV)
${}_{92}^{238}\text{U}$	$2s_{1/2}$	$8.8 \times 10^{-3}$	$5.4 \times 10^{-2}$
	$2p_{1/2}$	$9.2 \times 10^{-3}$	1.58
	$2p_{3/2}$	$2.7 \times 10^{-3}$	1.16
${}_{90}^{232}\text{Th}$	$2s_{1/2}$	$5.9 \times 10^{-3}$	$2.0 \times 10^{-2}$
	$2p_{1/2}$	$7.7 \times 10^{-3}$	$6.5 \times 10^{-1}$
	$2p_{3/2}$	$2.6 \times 10^{-3}$	$5.5 \times 10^{-1}$

Table 3. Mean lifetimes for the first nuclear excited states of  ${}_{92}^{238}\text{U}$  and  ${}_{90}^{232}\text{Th}$ . In the second column,  $\tau_{\text{neutral}}$  stands for the mean lifetime corresponding to the nucleus of a neutral atom, while the third column contains the values  $\tau_{\text{rad}}$  for the bare ion or H-like ion with the electron in the ground state. In the last column we present nuclear mean-lives of Li-like ( $2s_{1/2}$ ), B-like ( $2p_{1/2}$ ) and N-like ( $2p_{3/2}$ ) ions in their electronic ground states.

$\frac{A}{Z}X$	$\tau_{\text{neutral}}$ (ps)	$\tau_{\text{rad}}$ (ns)	$nl_j$	$\tau_{nl_j}$ (ns)
${}_{92}^{238}\text{U}$	292	185	$2s_{1/2}$	36.2
			$2p_{1/2}$	1.54
			$2p_{3/2}$	0.67
${}_{90}^{232}\text{Th}$	497	150	$2s_{1/2}$	50.1
			$2p_{1/2}$	2.35
			$2p_{3/2}$	1.04

states of the considered nuclei. In bare ions or H-like ions the NEECX process prolongs the lifetime  $\tau_{rad}$  to about 150 ns.

In conclusion, our theoretical calculations show that the fast electronic x-ray decay following the resonant electron capture leads to an essential increase of the resonance strength and of the lifetime of the excited nuclear state. These facts can serve to facilitate the measurement of the NEECX process at GSI with the present equipment.

## References

1. C. Brandau, C. Kozhuharov, A. Müller *et al.*, *Rad. Phys. and Chem.* **75**, 1763 (2006).
2. C. Brandau, C. Kozhuharov, Z. Harman *et al.*, *Phys. Rev. Lett.* **100**, 073201 (2008).
3. A. Pálffy *et al.*, *Phys. Rev. A* **73**, 012715 (2006).
4. A. Pálffy *et al.*, *Phys. Rev. A* **75**, 012709 (2007).
5. A. Pálffy *et al.*, *Phys. Rev. A* **75**, 012712 (2007).
6. A. Pálffy *et al.*, *Phys. Lett. B* **661**, 330 (2008).
7. P. Zimmermann *et al.*, *J. Phys. B: At. Mol. Phys.* **30**, 5259 (1997).
8. K. G. Dyall, I. P. Grant *et al.*, *Comput. Phys. Commun.* **55**, 425 (1989).
9. P. Zimmerer *et al.*, *Phys. Lett. A* **148**, 457 (1990).
10. X. Ma *et al.*, *Phys. Rev. A* **68**, 042712 (2003).
11. S. Zakowicz *et al.*, *Phys. Rev. A* **68**, 042711 (2003).
12. R. Schioppa *et al.*, *Eur. Phys. J. D* **31**, 21 (2004).